

# ONE STEP SYNTHESIS OF WATER-DISPERSIBLE $\text{CoFe}_2\text{O}_4$ MAGNETIC NANOPARTICLES USING TRIETHYLENETETRAMINE AS SOLVENT AND STABILISING LIGAND

Kieu T. B. Ngoc<sup>1</sup>, Phạm V. Luyen<sup>2</sup>, Nguyen C. Khang<sup>1</sup>, Pham H. Nam<sup>3</sup>,  
Do H. Manh<sup>3</sup>, Pham V. Vinh<sup>2</sup>, Pham V. Hung<sup>2</sup>, Le T. Lu<sup>4,\*</sup>

<sup>1</sup>*Nano Center-Hanoi University of Education, 136 Xuan Thuy, Cau Giay, Hanoi*

<sup>2</sup>*Faculty of Physics, Hanoi University of Education, 136 Xuan Thuy-Cau Giay, Hanoi*

<sup>3</sup>*Institute of Materials Science-VAST, 18 Hoang Quoc Viet, Cau Giay, Hanoi*

<sup>4</sup>*Institute for Tropical Technology-VAST, 18 Hoang Quoc Viet, Cau Giay, Hanoi*

\*Email: [ltlu\\_itims@yahoo.com](mailto:ltlu_itims@yahoo.com)

Received: 30 March 2015; Accepted for publication: 12 July 2015

## ABSTRACT

Magnetic  $\text{CoFe}_2\text{O}_4$  nanoparticles were synthesised by one step synthetic method through thermal decomposition of Co and Fe precursors in triethylenetetramine solvent at high temperature. The advantage of this method is the ability to make monodisperse nanoparticles with high water-dispersibility and stability. The particle size can be tuned in the range of 7-11.3 nm by varying synthetic conditions. The obtained particles with small DLS size (less than 21 nm) are ready to disperse and stable in aqueous solution for weeks without any surface modification.

*Keywords:* magnetic nanoparticles, water-dispersible, biomedicine, one step synthetic method.

## 1. INTRODUCTION

Magnetic nanomaterials have widely received attentions due to their diverse applications in the fields such as information technology [1], environmental treatment [2], catalysis [3, 4] and particularly in biomedicine [5]. In biomedicine, the magnetic nanoparticles can be used for biological separation, targeted drug delivery, or as contrast enhancers for magnetic resonance imaging (MRI) [6]. To date, synthetic strategies of nanoparticles in organic solvents at elevated temperatures under the presence of hydrophobic surfactant(s) are widely used for their ability to prepare monodisperse nanoparticles with good control over the size, shape and monodispersibility [6, 7]. However, as the hydrophobic nature of the surfactants, nanoparticles prepared by these techniques disperse only in non-polar solvent, which hinders them for biological applications. Transferring these hydrophobic particles into aqueous solution is still a major challenge.

Recently, several studies have introduced a new approach for the synthesis of water-dispersible magnetic nanoparticles [8]. In those studies, instead of using the non-polar solvent such as phenylether, benzylether, octadecene or dioctylether combined with hydrophobic surfactants (oleic acid, oleylamine or triphosphine oxide). The authors have used polar solvents with high boiling points, such as dimethylsulfoxide (DMSO), triethyleneglycol (TEG) or triethylenetetramine (TETA) as synthetic solvents [8]. In the two latter cases, in addition to the usual role as solvents, TEG and TETA molecules also serve as stabilizing ligands for suspending nanoparticles in aqueous solution. For example, O'Connor and colleagues reported their study on the synthesis of hydrophilic  $\text{Fe}_3\text{O}_4$  nanoparticles in TETA solvent at high temperatures [8]. In their work, the size of nanoparticles was controlled in the range of 7.4-12 nm using seeding growth method. The obtained nanoparticles are ready water-dispersible and stable without any further surface modification. Thus far, there are limited works on using TETA as solvent for synthesis of magnetic nanoparticles and these studies are only for  $\text{Fe}_3\text{O}_4$  nanomaterials. In our best knowledge, there are no reports on the synthesis of other magnetic nanomaterials (for example  $\text{CoFe}_2\text{O}_4$ ) in TETA recorded.

In the current work, water-dispersible and monodisperse  $\text{CoFe}_2\text{O}_4$  nanoparticles were prepared by thermal decomposition of cobalt (II) and iron (III) acetylacetonates in TETA solvent. The influence of the reaction time and precursor concentration on the morphology, monodispersity and magnetic nanoparticles was investigated. Analytical techniques, including transmission electron microscopy (TEM), vibrating sample magnetometer (VSM) and dynamic light scattering (DLS) were used to characterise the samples.

## 2. EXPERIMENTAL

### 2.1. Chemicals

All chemicals, including precursors: Co (II) acetylacetonate ( $\text{Co}(\text{acac})_2$ , 99 %), Fe (III) acetylacetonate ( $\text{Fe}(\text{acac})_3$ , 99.99 %); solvents: triethylenetetramine (TETA,  $\geq 97$  %), acetone and ethanol were ordered from Sigma-Aldrich Ltd, Singapore. They were used as received without any further purification.

### 2.2. Synthesis of $\text{CoFe}_2\text{O}_4$ nanoparticles

The syntheses of  $\text{CoFe}_2\text{O}_4$  nanoparticles were conducted under free oxygen condition. In a typical synthesis, 0.84 mmol  $\text{Co}(\text{acac})_2$  (0.213 g) and 1.68 mmol  $\text{Fe}(\text{acac})_3$  (0.6 g) were precisely weighed and stored in a three-necked flask containing 40 ml of TETA. The concentrations of the precursors  $\text{Co}(\text{acac})_2$  and  $\text{Fe}(\text{acac})_3$  in the reaction solution are 21 mM and 42 mM, respectively. The reaction mixture was magnetically stirred and de-gassed at room temperature for at least 30 min before heating to 100 °C, and maintained at this temperature to remove water. Temperature continued to be increased to 275 - 280 °C with a ramping rate of 3 - 5 °C/min. At this temperature, the reaction was maintained for various time periods of 30, 60 and 120 min.

### 2.3. Samples purification

As-synthesised  $\text{CoFe}_2\text{O}_4$  nanoparticles were purified from free excess surfactants or reaction by-products before characterisations. The purification of samples for TEM and DLS measurements was carried out as follows: 0.5 mL of the nanoparticle solution was mixed with 1

mL of acetone. The mixture was sonicated for 1 - 2 min and the nanoparticles were precipitated by a centrifugation at a speed between 5000 - 10000 rpm for 5 min (depending on the particle size). After discarding the supernatant, the nanoparticles were dissolved in 1 mL of water and then mixed with 2 mL acetone, following a further centrifugation. The precipitation-redispersion procedure was repeated three more times, and the nanoparticles were finally dissolved in 1.5 mL of water prior to TEM and DLS characterizations. The washing procedure of samples for XRD and VSM measurements was conducted similarly to that of TEM characterization but using larger sample volume (5 - 10 mL sample solution/each) and the purified samples were dried, instead of dispersing in water.

### 3. RESULTS AND DISCUSSION

#### 3.1. Effect of reaction time on the monodispersity and size of the nanoparticle

It was widely known that the size, shape and monodispersibility of nanoparticles can be controlled by synthetic conditions. In this study, we investigated the influence of the reaction time to the morphology and uniformity of the particle. Figure 1 shows TEM images and corresponding size distribution histograms of the samples synthesised at different reaction time periods (30, 60 and 120 min). At the reaction time duration of 30 min, it can be seen that most of the obtained nanoparticles are spherical- and cubic-shaped with an average size  $d = 9.5 \pm 1.4$  nm. As the reaction time duration increased to 60 min, the particle size increased to  $11.3 \pm 1.6$  nm. Continued to prolong the reaction time to 120 min, we observed a decrease in particle size ( $d = 10.5 \pm 1.7$  nm). From TEM analysis results (size distribution histograms), it can be seen that CoFe<sub>2</sub>O<sub>4</sub> nanoparticles synthesised within 30 - 120 min reaction time periods are fairly uniform (stdev  $\approx$  15 - 17 %).

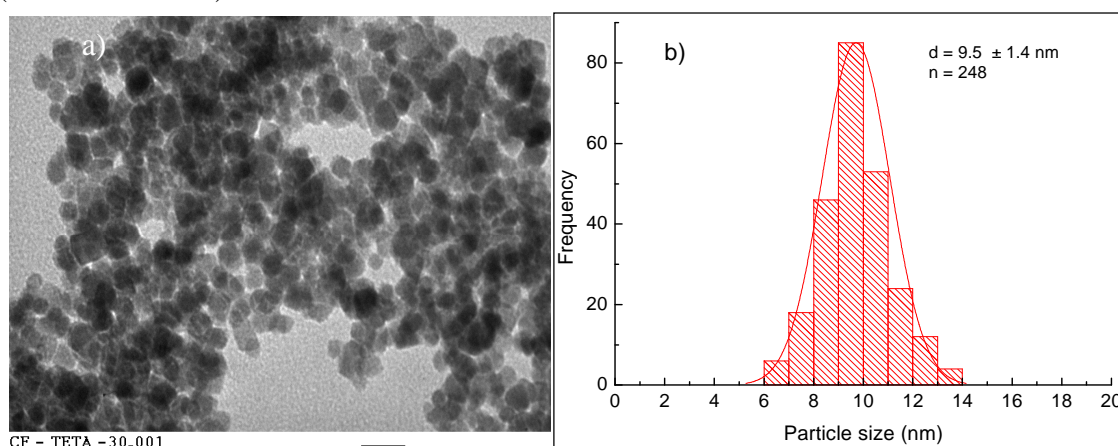


*Figure 1.* TEM images and corresponding size distribution histograms of the CoFe<sub>2</sub>O<sub>4</sub> nanoparticles synthesised for different reaction time periods: 30 min (a, b).

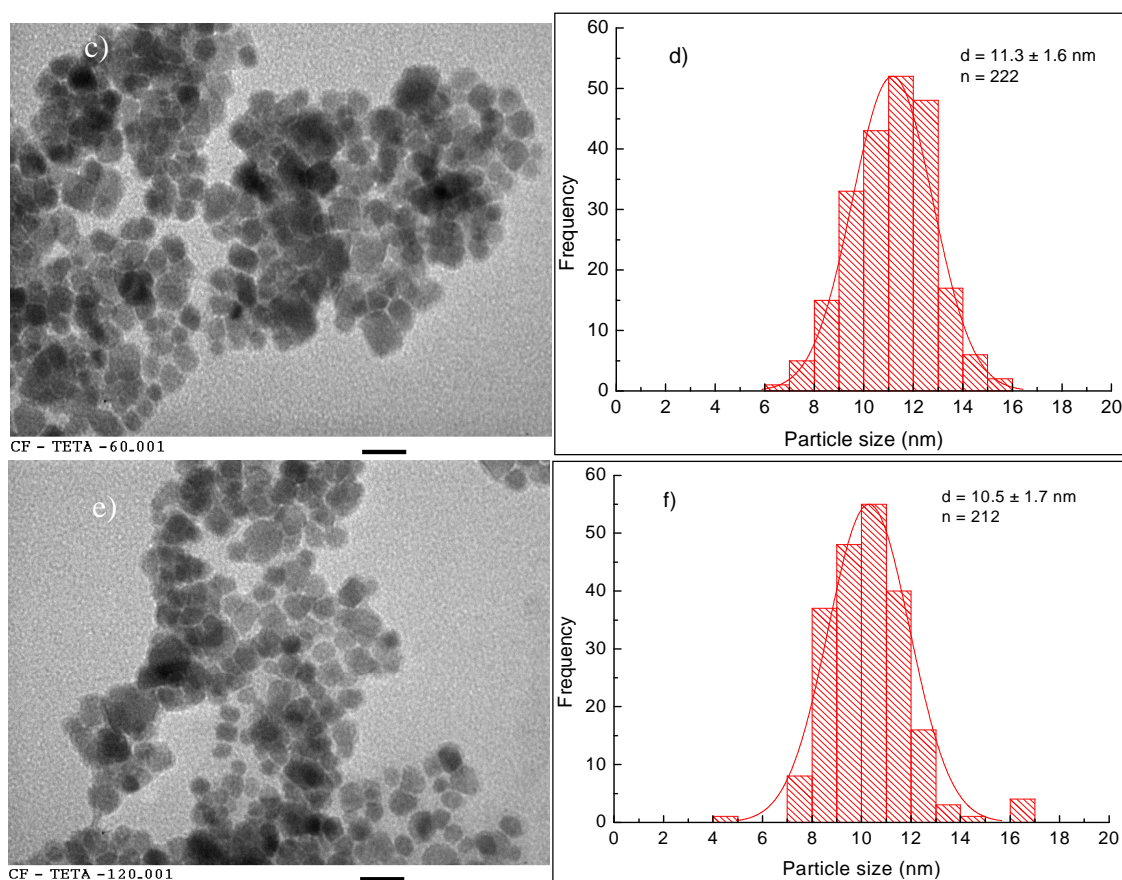


Figure 1. TEM images and corresponding size distribution histograms of the  $\text{CoFe}_2\text{O}_4$  nanoparticles synthesised for different reaction time periods: 60 min (c,d) and 120 min (e, f). Scale bar of a, c and e images: 20 nm.

### 3.2. The influence of the precursor concentration on the size and uniform of $\text{CoFe}_2\text{O}_4$ nanoparticles

To investigate the influence of the  $\text{Co}(\text{acac})_2$  and  $\text{Fe}(\text{acac})_3$  concentration on the formation, size and uniform of  $\text{CoFe}_2\text{O}_4$  nanoparticles, we maintained the reaction time duration at 30 min while changing concentration of the precursors. TEM data in Figure 1a,b and 2a,b indicated that when the concentration of precursors was doubled, from 21 mM  $\text{Co}^{2+}$  + 42 mM  $\text{Fe}^{3+}$  to 42 mM  $\text{Co}^{2+}$  + 84 mM  $\text{Fe}^{3+}$ , the particles size was reduced from  $9.5 \pm 1.4$  nm to  $7.2 \pm 0.8$  nm, respectively. Continued to increase the precursor concentration to 84 mM  $\text{Co}^{2+}$  + 168 mM  $\text{Fe}^{3+}$ , we obtained the particles size of  $10.5 \pm 1.8$  nm. Along with the change of the particle size, monodispersity of the synthesised  $\text{CoFe}_2\text{O}_4$  nanoparticles also altered with varying the concentration of the precursors. For example, the value of standard deviation (stdev) of the nanoparticles was improve from stdev = 16 %, for sample prepared at precursor concentration of 21 mM  $\text{Co}^{2+}$  and 42 mM  $\text{Fe}^{3+}$  (Figure 1a, b), to  $\approx 11$  %, for the sample synthesised at 42 mM  $\text{Co}^{2+}$  + 84 mM  $\text{Fe}^{3+}$  (Figure 2a, b).

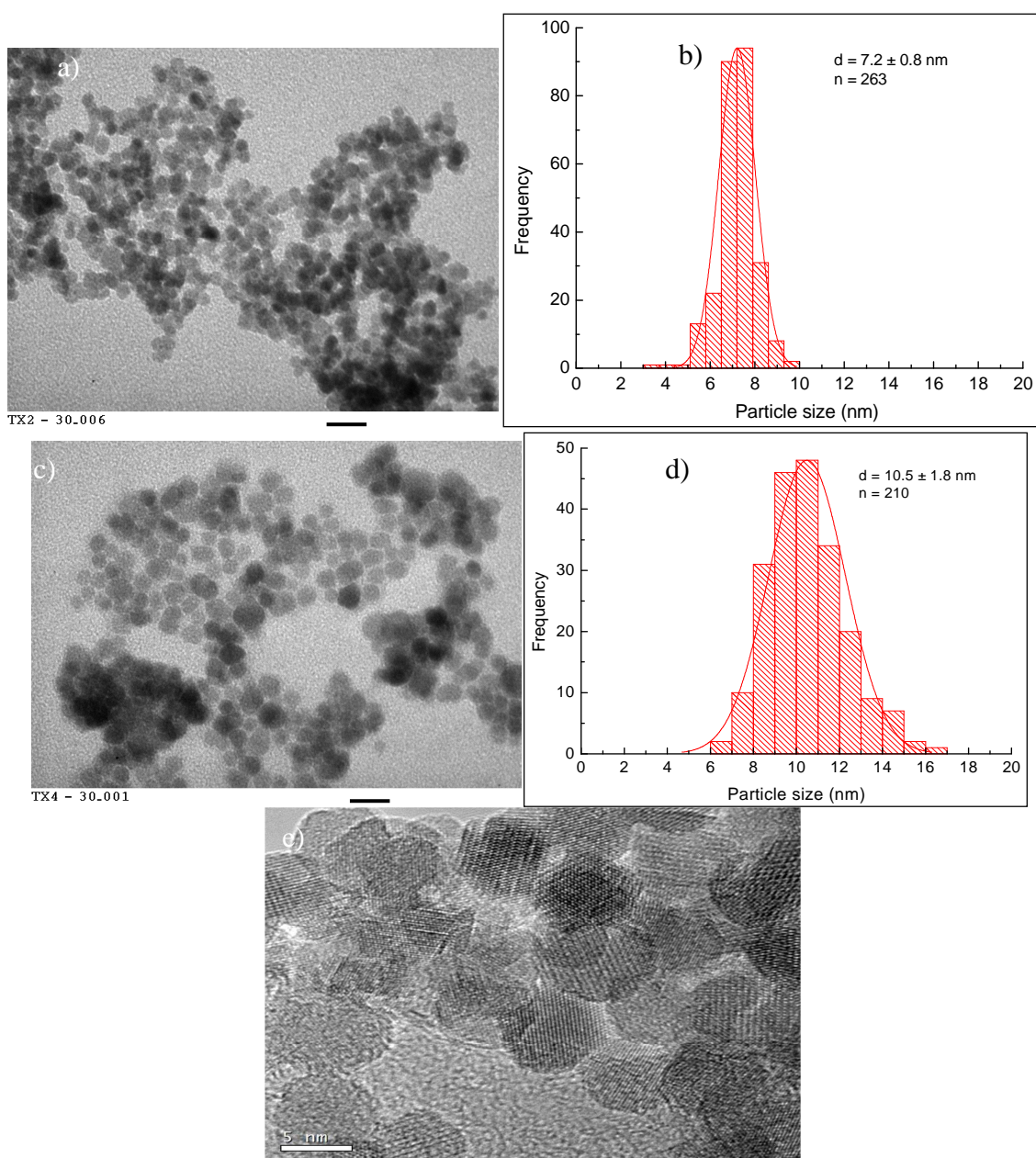


Figure 2. TEM images and corresponding size distributions histograms of  $\text{CoFe}_2\text{O}_4$  nanoparticles synthesised at different precursor concentrations ( $\text{mM Co}^{2+} + \text{mM Fe}^{3+}$ ): 42 + 84 (a,b), 84 + 168 (c,d). e) HRTEM image of (a). The reaction time duration is 30 min. Scale bar of a and c images: 20 nm.

This value is nearly equivalent to that of the sample prepared in dioctylether or octadecene in our previous works, suggesting the high quality of the  $\text{CoFe}_2\text{O}_4$  nanoparticles synthesised in TETA. We also conducted some high resolution TEM analyses (HRTEM) to explore the level of crystallinity of the samples. Figure 2e indicates HRTEM image of the sample synthesised at the concentration of 42  $\text{mM Co}^{2+}$  and 84  $\text{mM Fe}^{3+}$ . One can see clearly the crystal lattices, which suggest a high crystallinity of the analysed sample. By analyzing the HRTEM image in more

detail, we determined the distances ( $d_{hkl}$ ) between crystal lattices are 2.526, 1.481 and 1.612 Å, which are corresponding to the planes of (311), (440) and (511), respectively. These results are consistent with the calculations obtained from the diffraction peak positions on the XRD patterns in Figure 3.

### 3.3. Phase structure of $\text{CoFe}_2\text{O}_4$ nanoparticles

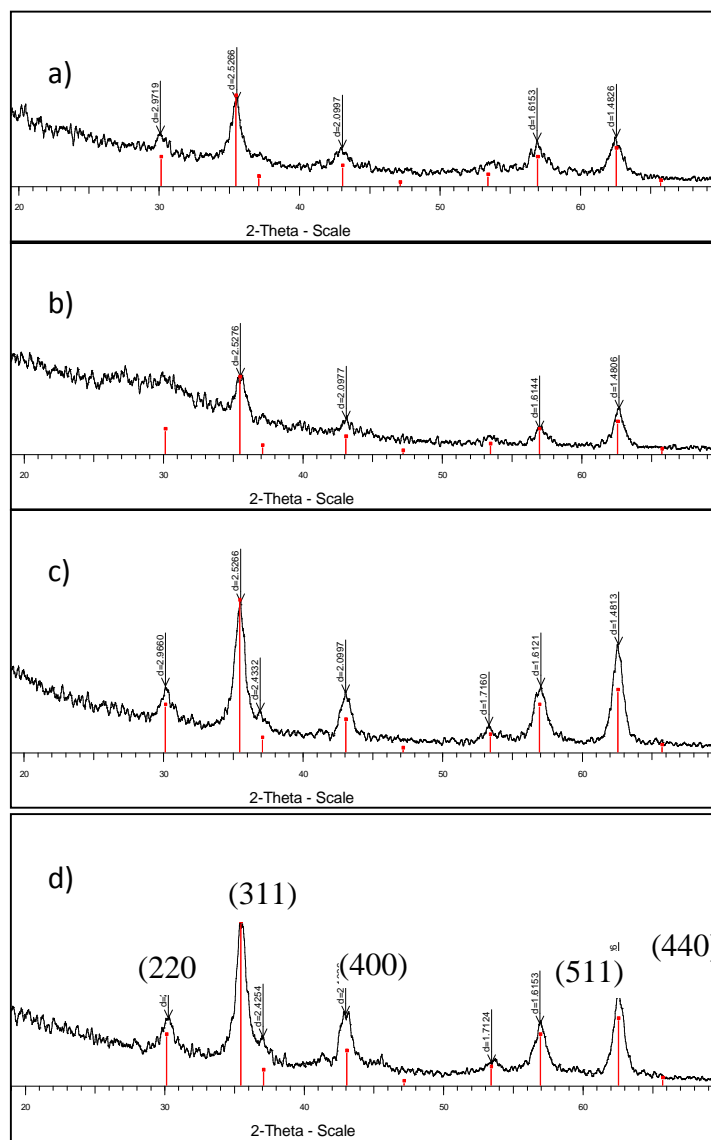


Figure 3. X-ray diffraction patterns of the  $\text{CoFe}_2\text{O}_4$  nanoparticles synthesised in TETA at different concentrations of precursors: a,b) 21 mM  $\text{Co}^{2+}$  + 42 mM  $\text{Fe}^{3+}$ , c) 42 mM  $\text{Co}^{2+}$  : 84 mM  $\text{Fe}^{3+}$  and d) 84 mM  $\text{Co}^{2+}$  : 168 mM  $\text{Fe}^{3+}$ . The reaction time durations are 30 min (a, c and d) and 120 min (b).

Figure 3 shows XRD patterns of the samples synthesised under different synthetic conditions. One can see that all samples exhibited the characteristic diffraction peaks of the spinel  $\text{CoFe}_2\text{O}_4$  phase, including (220), (311), (400), (511) and (440). Of these, the peak (311)

had the strongest intensity. There were no characteristic peaks of Fe<sub>2</sub>O<sub>3</sub>, FeO or CoO phases detected in the XRD patterns, which demonstrated that the prepared samples are single phase spinel structure. In addition, we observed that the full width at half-maximum of the strongest (311) peak of the samples prepared at different synthetic conditions differed insignificantly, which indicates that the particle size changed in a small range within the studied conditions. This result is consistent with the TEM data in the Figure 1 and 2, where the particle size can vary just in the range of 7.2 - 10.5 nm by changing the precursor concentration.

### 3.4. Magnetic properties of the CoFe<sub>2</sub>O<sub>4</sub> nanoparticles

The field-dependent magnetization measurements of the samples were carried out on vibrating sample magnetometer, VSM. Figure 4 shows the hysteresis curves of some samples measured at room temperature. All these loops show no remanence nor coercivity ( $H_c = 0$  and  $M_r = 0$ ), which suggest a superparamagnetic state of the samples. With all studied samples, the magnetization value,  $M_s = 40 \div 57$  emu/g, is significantly smaller than that of bulk CoFe<sub>2</sub>O<sub>4</sub> material (70 - 80 emu/g). This reduction of the magnetization value can be explained due to the influence of spin canting effect (disorder of the surface magnetic moment).

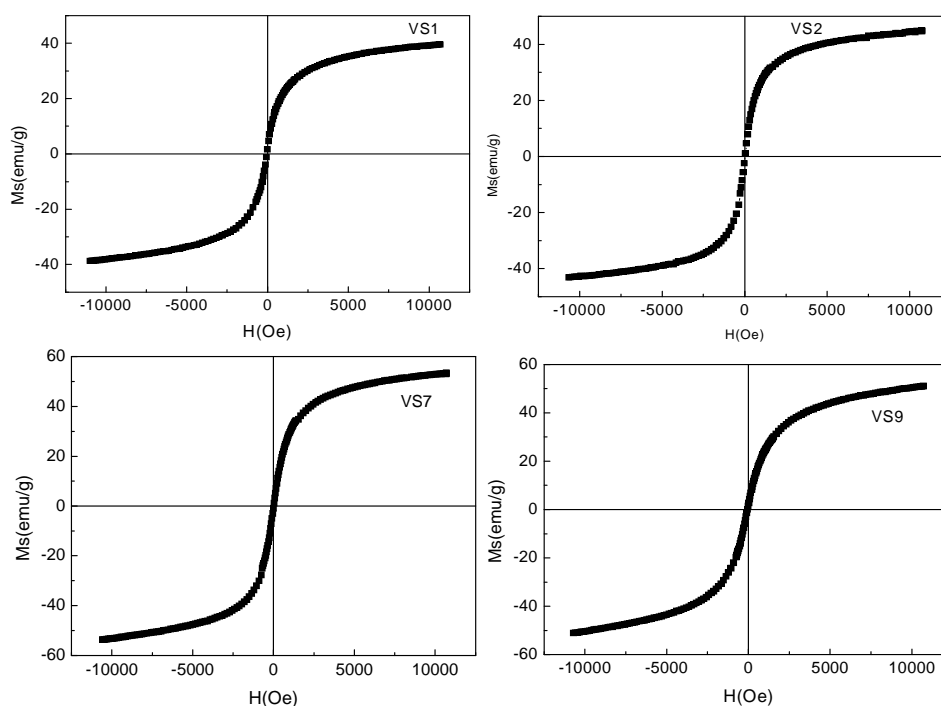


Figure 4. The magnetisation loops of CoFe<sub>2</sub>O<sub>4</sub> nanoparticles synthesised at concentrations of precursors of 21 mM Co<sup>2+</sup> + 42 mM Fe<sup>3+</sup> for different reaction time durations: 30 min (VS1), 60 min (VS7) and 120 min (VS9), and concentration of 42 mM Co<sup>2+</sup> + 84 mM Fe<sup>3+</sup> for 30 min (VS2).

### 3.5. Water-dispersibility of CoFe<sub>2</sub>O<sub>4</sub> nanoparticles

To use the synthesised nanoparticles for the biomedical application purposes, we have assessed the colloidal stability and water-dispersibility of the nanoparticles. Figure 5 shows the DLS spectra of the samples in water synthesised at the different reaction time durations. On DLS spectra, we obtained peaks at 14, 18.5 and 20.5 nm for the samples prepared at the reaction time

durations of 30, 120 and 60 min, respectively. The obtained DLS data suggested that the prepared nanoparticles are very good dispersion in water without any agglomeration and precipitation. The well aqueous dispersion of  $\text{CoFe}_2\text{O}_4$  nanoparticles synthesised in TETA solvent is explained primarily due to the strong bond of TETA molecules to the surface of  $\text{CoFe}_2\text{O}_4$  nanoparticles through amine ( $\text{NH}_2$ ) functional group. During the growth process of  $\text{CoFe}_2\text{O}_4$  nanoparticles at high temperature, TETA molecules attach to the particle surface to form a robust ligand shell wrapped around the forming nanoparticles. This ligand shell, on the one hand, inhibits the growth of the nanoparticles (control the size), on the other hand, it protects nanoparticles from agglomerations via steric repulsion and thus helps them to disperse well in solution. Furthermore, due to the hydrophilic nature of the ligand molecules, the TETA capped  $\text{CoFe}_2\text{O}_4$  nanoparticles are readily dispersible in aqueous solvent without further surface modification steps.

We were also evaluated the colloidal stability of the samples through visual observation. Figure 5 shows snapshots of a diluted sample solution in water (middle picture) and in a mixture of hexane/water (left picture). We observed that the nanoparticles dispersed very well in water but absolutely not dispersed in hexane. Two weeks after dispersing them in water, an insignificant amount of agglomeration and precipitation of the nanoparticles was observed. In the case of nanoparticles dispersed in the mixture of hexane/water, the nanoparticles transferred quickly into the water phase after shaking just about one min.

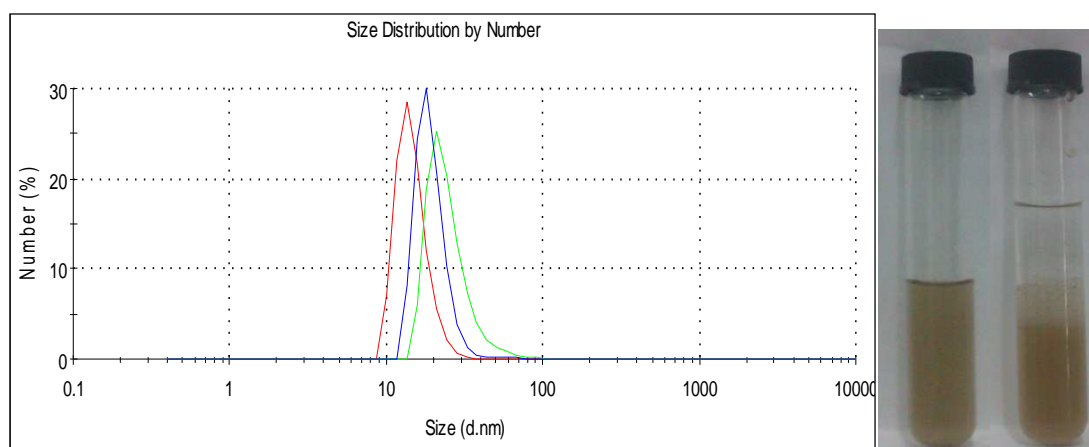


*Figure 5.* DLS spectra (left panel) of aqueous solution containing  $\text{CoFe}_2\text{O}_4$  nanoparticles synthesised for different reaction time durations: 30 (red), 60 (green) and 120 min (blue), and photos of solution of the nanoparticles dispersed in water (middle picture) and in a mixture of hexane/water (left picture). Hexane is light and rises above water.

#### 4. CONCLUSION

We have successfully prepared monodisperse and water-dispersible  $\text{CoFe}_2\text{O}_4$  nanoparticles using one step synthetic method. The prepared nanoparticles are readily dispersible and relatively stable in aqueous solution without further surface modification steps. The particle size can be varied in the range of 7.2 - 11.3 nm with a standard deviation up to 11%. XRD and VSM data indicated that obtained nanoparticles are single phase and superparamagnetic at room temperature with the highest saturation magnetization of  $\approx 60$  emu/g. The well dispersion and relatively stability in water of monodisperse  $\text{CoFe}_2\text{O}_4$  nanoparticles possibly opens up several

potential applications in biomedicine, including hyperthermal cancer treatment and magnetic resonance imaging MRI.

**Acknowledgements.** This work was financially supported by the National Foundation for Science and Technology Development, NAFOSTED (grant: 103.02-2012.74) and partly supported by VAST (grant: VAST.DLT.04/12-13).

## REFERENCES

1. Sekitani T., Yokota T., Zschieschang U., Klauk H., Bauer S., Takeuchi K., Takamiya M., Sakurai T., and Someya T. - Organic nonvolatile memory transistors for flexible sensor arrays, *Science* **326** (2009) 1516–1519.
2. Nainani R., Thakur P., Chaskar M. - Synthesis of Silver Doped TiO<sub>2</sub> Nanoparticles for the Improved Photocatalytic Degradation of Methyl Orange, *J. Materials Sci. and Engineering B* **2** (1) (2012) 52-58.
3. Magrez A., Seo J. W., Miko C., Hernardi K., Forro L. - Growth of Carbon Nanotubes With Alkaline Earth Carbonate as Support, *J. Phys. Chem.* **109** (2005) 10087-10091.
4. Magrez A., Seo J. W., Smajda R., Mionic M. & Forro L. - Catalytic CVD Synthesis of Carbon Nanotubes: Towards High Yield and Low Temperature Growth, *Materials* **3** (2010) 4871-4891.
5. Lu A. H., Salabas E. L., and Schüth F. - Magnetic Nanoparticles: Synthesis, Protection, Functionalization, and Application, *Angew. Chem. Int. Ed.* **8** (2007) 1222-1244.
6. Puentes V. F., Krishnan K. M., and Alivisatos A. P. - Colloidal nanocrystal shape and size control: the case of cobalt, *Science* **291** (2001) 2115-2117.
7. Park J., Lee E., Hwang N. M., Kang M. S., Kim S. C., Hwang Y., Park J. G., Noh H. J., Kini J. Y., Park J. H., Hyeon T. - One-nanometer-scale size-controlled synthesis of monodisperse magnetic Iron oxide nanoparticles, *Angew. Chem. Int. Ed.* **117** (2005) 2932-2937.
8. Qu H., Ma H., Riviere A., Zhou W. and O'Connor C. J. - One-pot Synthesis in Polyamines for Preparation of Water-soluble Magnetite Nanoparticles with Amine Surface Reactivity, *J. Mater. Chem.* **22** (2012) 3311-3313.
9. Li Z., Wei L., Gao M. Y., Lei H. - One-pot reaction to synthesize biocompatible magnetite nanoparticles, *Adv. Mater.* **17**(2005) 1001-1005.
10. Hu F., Li Z., Tu C., Gao M. - Preparation of magnetite nanocrystals with surface reactive moieties by one-pot reaction, *J. Colloid Interface Sci.* **311**(2007) 469-474.
11. Zhang T., Ge J., Hu Y. and Yin Y. - A General Approach for Transferring Hydrophobic Nanocrystals into Water, *Nano. Lett.* **7**(2007) 3203-3207.
12. Liu Y., Chen T., Wu C., Qiu L., Hu R., Li J., Cansiz S., Zhang L., Cui C., Zhu G., You M., Zhang T. and Tan W. - Facile Surface Functionalization of hydrophobic Magnetic Nanoparticles, *JACS.* **136** (2014) 12552-12555.
13. Palma R. D., Peeters S., Van Bael M. J., Van den Rul H., Bonroy K., Laureyn W., Mullens J., Borghs G. and Maes G. - Silane Ligand Exchange to Make Hydrophobic Superparamagnetic Nanoparticles Water-Dispersible, *Chem. Mater.* **19** (2007) 1821-1831.

14. Kim J., Kim H. S., Lee N., Kim T., Kim H., Yu T., Song I. C., Moon W. K. and Hyeon T. - Multifunctional Uniform Nanoparticles Composed of a Magnetite Nanocrystal Core and a Mesoporous Silica Shell for Magnetic Resonance and Fluorescence Imaging and for Drug Delivery, *Angew. Chem. Int. Ed.* **47** (2008) 8438–8444.
15. Deng Y., Qi D., Deng C., Zhang X. and Zhao D. - Superparamagnetic High-Magnetization Microspheres with an  $\text{Fe}_3\text{O}_4@ \text{SiO}_2$  Core and Perpendicularly Aligned Mesoporous  $\text{SiO}_2$  Shell for Removal of Microcystins, *JACS.* **130** (2008) 28-29.
16. Selvan S. T., Patra P. K., Ang C. Y. and Ying J. Y. - Synthesis of silica-coated semiconductor and magnetic quantum dots and their use in the imaging of live cells, *Angew. Chem. Int. Ed.* **46** (2013) 2448-2452.

## TÓM TẮT

### CHẾ TẠO HẠT NANO TỪ $\text{CoFe}_2\text{O}_4$ CÓ KHẢ NĂNG PHÂN TÁN TRONG NƯỚC THEO QUY TRÌNH MỘT BƯỚC SỬ DỤNG DUNG MÔI TRIETHYLENETETRAMIN

Kiều T. B. Ngọc<sup>1</sup>, Phạm V. Luyên<sup>2</sup>, Nguyễn C. Khang<sup>1</sup>, Phạm H. Nam<sup>3</sup>, Đỗ H. Mạnh<sup>3</sup>,  
Phạm V. Vĩnh<sup>2</sup>, Phạm V. Hùng<sup>2</sup>, Lê T. Lư<sup>4,\*</sup>

<sup>1</sup>*Trung tâm Nano, Trường ĐHSP Hà Nội, 136 Xuân Thủy, Cầu Giấy, Hà Nội*

<sup>2</sup>*Khoa Vật lý, Trường ĐHSP Hà Nội, 136 Xuân Thủy, Cầu Giấy, Hà Nội*

<sup>3</sup>*Viện Khoa học vật liệu, Viện HLKHCNVN, 18 Hoàng Quốc Việt, Cầu Giấy, Hà Nội*

<sup>4</sup>*Viện Kỹ thuật nhiệt đới, VAST, 18 Hoàng Quốc Việt, Cầu Giấy, Hà Nội*

\*Email: [ltlu\\_itims@yahoo.com](mailto:ltlu_itims@yahoo.com)

Hạt nano từ  $\text{CoFe}_2\text{O}_4$  đã được tổng hợp thành công bằng phương pháp chế tạo một bước qua việc phân hủy các tiền chất của Co và Fe trong dung môi triethylenetetramin ở nhiệt độ cao. Ưu điểm của phương pháp này là cho phép tạo ra các hạt nano từ đồng đều với khả năng phân tán tốt và bền trong nước. Kích thước hạt có thể điều khiển trong khoảng 7 - 11,3 nm bằng cách thay đổi điều kiện phản ứng. Các hạt thu được có bán kính động (DLS) tương đối nhỏ ( $\leq 21$  nm), dễ dàng phân tán và bền trong nước trong thời gian lên tới vài tuần mà không cần bất kì một công đoạn biến tính bề mặt nào khác.

*Từ khóa:* hạt nano từ, phân tán trong nước, y sinh, phương pháp tổng hợp một bước.